

Article

Soot Nanoparticles Could Partake in Nucleation of Biogenic Particles in the Atmosphere: Using Fullerene as a Model Compound

Yiwen Liu ¹, Zhuang Wang ^{1,*}, Se Wang ^{1,*}, Hao Fang ¹ and Degao Wang ²

¹ Collaborative Innovation Center of Atmospheric Environment and Equipment Technology (AEET), Jiangsu Key Laboratory of Atmospheric Environment Monitoring and Pollution Control (AEMPC), School of Environmental Science and Engineering, Nanjing University of Information Science and Technology, Nanjing 210044, China; yiwenu20@163.com (Y.L.); fh@nuist.edu.cn (H.F.)

² Department of Environmental Science and Engineering, Dalian Maritime University, Dalian 116026, China; degaowang@163.com

* Correspondence: zhuang.wang@nuist.edu.cn (Z.W.); wangse@nuist.edu.cn (S.W.); Tel.: +86-25-5873-1090 (Z.W. & S.W.)

Academic Editor: Robert W. Talbot

Received: 3 February 2016; Accepted: 3 February 2016; Published: 14 March 2016

Abstract: The detection of existence of fullerenes (C₆₀ and C₇₀) makes it necessary to explore whether soot nanoparticles can participate in new nanometer-sized particle formation and growth in the atmosphere. This study describes a theoretical investigation at multiple levels on the role of the fullerenes (as model compounds to represent nanoparticles of soot) in the formation of complexes with a common atmospheric nucleating precursor (sulfuric acid, SA) and a biogenic organic acid (cis-pinonic acid, CPA), as well as initial growth of nano-sized biogenic aerosols. Quantum chemical density-functional theory calculations identify the formation of stable fullerene-[CPA-SA] ternary complexes, which likely leads to an enhanced nucleation of SA with CPA. Relevant thermochemical parameters including the changes of Gibbs free energy, enthalpy, and entropy for the complex formation also support that fullerene-[CPA-SA] is most likely to be a newly formed nuclei. The sizes of the critical nucleus of the fullerene-[CPA-SA-H₂O] systems were found to be approximately 1.3 nm by large-scale molecular dynamics simulations. This study may provide a new insight into the mechanisms underlying the formation of new particle in the atmospheric environment.

Keywords: fullerenes; biogenic particles; nucleation; growth; molecular simulation

1. Introduction

New particle formation is an important process affecting the properties of aerosols in the atmospheric environment [1,2]. New particle formation can be divided into two main processes [3]. The first part is nucleating, and the second part is the growth of the nucleus. Due to its low saturated vapor pressure, SA is considered to be a critical species for new particle formation [4]. It is commonly recognized that binary nucleation theory is not sufficient to explain atmospheric new particle formation, which likely implies participation of other species in nucleation, in addition to SA [1,2,5].

To date, the production of nanomaterials has increased vigorously, resulting in the high probability of occurrence of nanoparticles in the atmosphere and toxic effects due to their incidental emissions from urban and industrial development [6–10]. Carbon-based nanomaterials with different types have been shown to appear in usual hydrocarbon flames and emitted from normal heat sources [11]. For example, Sanchís *et al.* [12] found that the median phase concentrations of C₆₀ and C₇₀ fullerenes aerosol were 0.06 and 0.48 ng/m³, respectively for the Mediterranean Sea atmosphere. Moreover, C₇₀ fullerene was the most frequently detected compound and it was also found in higher concentrations

for most samples, reaching 233.8 ng/m^3 [12]. It is reasonable to believe that soot nanoparticles occur ubiquitously in the atmosphere. Therefore, urgent attention and consideration are needed to investigate whether soot nanoparticles can partake in the formation of new atmospheric particles.

In the present study, we provided a theoretical description of the possible involvement of fullerene (C_{60} or C_{70}) seeds in atmospheric new particle formation. The fullerenes as model compounds to represent nanoparticles of soot can provide certain evidence for the growing importance of soot and the more general absorbing aerosol varieties of black and brown carbon in the atmosphere. Based on the Local Density Approximation (LDA) and Generalized Gradient Approximation with Dispersion-corrected Density-Functional Theory (GGA+DFT-D) methods, optimized geometries of Cis-Pinonic Acid-Sulfuric Acid (CPA-SA) and the combination with the C_{60} and C_{70} seeds are achieved. In addition, binding energy (E_B) and thermochemical parameters have been calculated to evaluate the stability of complexes. Furthermore, we characterized the sizes of the critical nucleus by large-scale Molecular Dynamics (MD) simulations.

2. Computational Methods

2.1. Density-Functional Theory Calculations

Forcite Plus code was used to obtain the initial optimized structures of the studied systems at a molecular mechanics level [13–16]. The atomic configuration with the lowest total energy for each system was built as a set of inputs for geometry optimization and properties calculation at a quantum mechanics level. All the quantum-chemical calculations were performed using the Dmol³ code in the Density-Functional Theory (DFT) framework. In this study, the LDA and the GGA+DFT-D methods were employed to calculate the isolated molecules and compounds. The chosen correction methods were used for the description of dispersive forces. The exchange-correlation potential was considered for the energy calculations in LDA with the Vosko–Wilk–Nusair functional [17] and in GGA with the Perdew, Burke, and Enzerhof functional [18]. The calculations were based on a double-numeric quality basis set with polarization functions.

2.2. MD Simulations

The critical nucleus sizes were simulated using full atomistic MD simulations in the NVT ensemble using the COMPASS force field, subjected to periodic boundary conditions in all three directions. For the non-bonding interactions, the Ewald method was used to calculate the electrostatic interactions, while the atom-based method was chosen to calculate the van der Waals energy with a cutoff of 9.5 \AA . Moreover, the MD simulations were performed at the temperature of 298.15 K . A simulation time of 1.0 ns was used to relax the system into equilibrium at a time step of 1 fs . All the calculations were performed with the Materials Studio 6.0 (Accelrys Inc.: San Diego, CA, USA).

2.3. Binding Energy Calculations

The value of binding energy (E_B) was utilized to estimate the stability of the complexes and the tendency of the formation process. A negative E_B value corresponded to a stable interaction between the components. E_B was calculated by:

$$E_B = E_{\text{complex}} - E_{\text{fullerene}} - E_{\text{CPA-SA}} \quad (1)$$

where E_{complex} , $E_{\text{fullerene}}$, and $E_{\text{CPA-SA}}$ refer to the total energy of the fullerene-[CPA-SA] complexes, the isolated fullerene, and the CPA-SA complex, respectively.

2.4. Thermodynamic Parameter Calculations

To compute changes in thermodynamic parameters, the computed thermodynamic parameter was added to the electronic energy of each component. For the fullerene-[CPA-SA] systems, Gibbs

free energy changes (ΔG), enthalpy changes (ΔH), and entropy changes (ΔS) were calculated by the following equations:

$$\Delta G = G_{\text{complex}} - G_{\text{fullerene}} - G_{\text{CPA-SA}} \quad (2)$$

$$\Delta H = H_{\text{complex}} - H_{\text{fullerene}} - H_{\text{CPA-SA}} \quad (3)$$

$$\Delta S = (\Delta H - \Delta G)/T \quad (4)$$

where H is the sum of electronic and thermal enthalpies and G is the sum of electronic and thermal free energies for the optimized configurations.

3. Results and Discussion

Based on the LDA and the GGA+DFT-D methods, optimized geometries of the CPA-SA complex and the combination with the C_{60} and C_{70} seeds were achieved. As shown in Table 1, for both the C_{60} -[CPA-SA] and C_{70} -[CPA-SA] systems, the E_B values are negative, indicating that the formed complexes are stable. The ΔG values are also negative, which implies that the formation process of the two systems is spontaneous. Moreover, the negative ΔH and ΔS values indicate that the two systems are exothermic and are not coincident. In addition, taking into account the values of $\Delta H < 0$ and $\Delta S < 0$, van der Waals interaction may mainly contribute to the driving force in these systems.

Table 1. Calculated parameters through density-functional theory for the model systems (1 atm, 298.15 K) ^a.

Model System	LDA				GGA+DFT-D			
	E_B	ΔG	ΔH	ΔS	E_B	ΔG	ΔH	ΔS
CPA-SA	-31.61	-21.67	-33.18	-38.60	-45.75	-29.20	-45.23	-53.76
C_{60} -[CPA-SA]	-14.03	-2.23	-13.18	-36.73	-24.85	-12.34	-22.27	-33.31
C_{70} -[CPA-SA]	-15.35	-1.10	-15.25	-47.46	-38.19	-28.73	-38.96	-34.31

^a E_B (kcal·mol⁻¹), ΔG (kcal·mol⁻¹), ΔH (kcal·mol⁻¹), and ΔS (cal·mol⁻¹·K⁻¹) are binding energy, changes in Gibbs free energy, enthalpy, and entropy, respectively.

Hydrogen bonds can be also a driving mechanism for the formation of the SA-organic acid complexes [19]. Based on the optimized structures obtained from the DFT methods, changes in hydrogen bond length for the CPA-SA complex were observed in the absence and presence of C_{60} and C_{70} (Figure 1). The addition of the double hydrogen bond length (2.589 Å) for the CPA-SA complex slightly decreases to 2.515 Å complexed by C_{60} and slightly decreases to 2.560 Å complexed by C_{70} , which can be judged from the LDA method (Figure 1A). Similar observation shows that the addition of the double hydrogen bond length (3.184 Å) for the CPA-SA complex slightly decreases to 3.114 Å complexed by C_{60} and slightly decreases to 3.161 Å complexed by C_{70} , which can be judged from the GGA+DFT-D method (Figure 1B). In general, the participation of C_{60} and C_{70} decreases the total hydrogen bond length and promotes the binding of the CPA-SA complex. Therefore, in light of the changes of the thermochemical properties and the hydrogen bond length, the C_{60} -[CPA-SA] and C_{70} -[CPA-SA] systems are likely to be a newly formed nucleus.

Figure 2 depicts the MD simulations of the critical nucleus of the CPA-SA-H₂O system in the absence and presence of the fullerenes. A previous study indicates that the critical nucleus likely consists of one CPA and three to five SA molecules along with several water (H₂O) molecules [20]. In this study, one CPA, four SA and ten H₂O molecules were selected to simulate the effects of the fullerenes on the nuclei sizes of the CPA-SA-H₂O system. The estimated sizes increased from 9.56 Å for the CPA-SA complex to 10.24 Å for the critical nucleus (CPA-SA-H₂O). It is obvious that the SA part of the complex is hydrophilic, corresponding exclusively to the growth of the cluster, while the CPA portion of the complex, which is hydrophobic, prevents interaction with additional molecules [20]. The estimated sizes of the C_{60} -[CPA-SA-H₂O] and C_{70} -[CPA-SA-H₂O] systems are 12.52 Å and 13.07 Å, respectively, which are significantly larger than the complex without the fullerenes. This implies that

the growth of the critical nucleus remains when the fullerenes are presented. As aforementioned, the fullerenes can interact with the CPA-SA complex though the fullerenes and CPA are both hydrophobic. Thus, the fullerenes may mitigate the inhibition effect of CPA on the cluster growth. It can be concluded that the fullerene seeds strongly influence the formation of terrestrial biogenic particles. In general, this study describes an important model compound (fullerene) for heterogeneous nucleation, and thus the results of this study can be used to stimulate further experimental and theoretical studies in this direction.

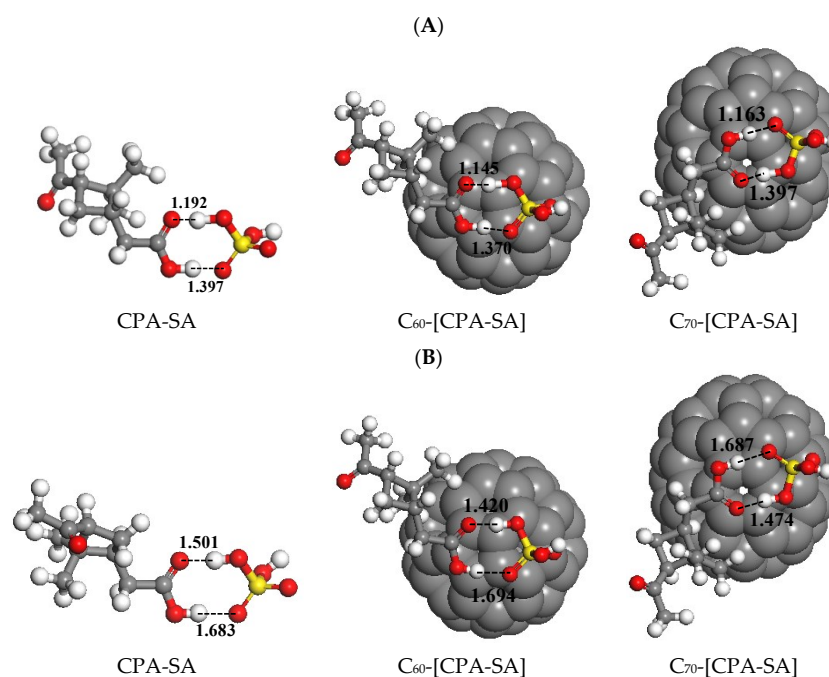


Figure 1. Optimized geometries of the complexes of Cis-Pinonic Acid (CPA), Sulfuric Acid (SA), and fullerenes (C₆₀ and C₇₀) at the LDA (A) and the GGA+DFT-D (B) levels.

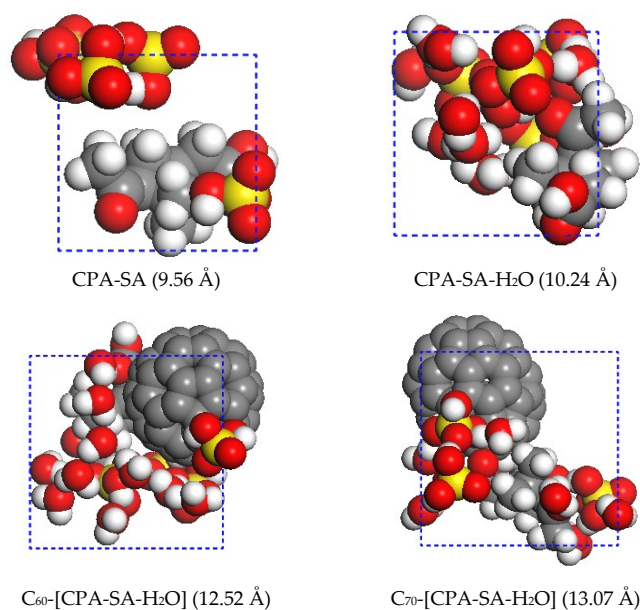


Figure 2. Molecular dynamic simulations of a critical nucleus consisting of one fullerene, one cis-pinonic acid (CPA), four sulfuric acid (SA), and 10 water (H₂O) molecules. Carbon, sulfur, oxygen, and hydrogen atoms are represented by black, yellow, red, and gray spheres, respectively.

4. Conclusions

Taking comprehensive account of the thermochemical changes and the hydrogen bond length changes from both the LDA and GGA+DFT-D methods, the participation of the C₆₀ and C₇₀ seeds is in favor of the formation of new atmospheric particles with the nuclei of the CPA-SA complex. The large-scale MD simulations suggest that the sizes of the critical nucleus of the fullerene-[CPA-SA-H₂O] systems were found to be approximately 1.3 nm. The strong interactions between soot nanoparticles and biogenic particles, as well as anthropogenic sulfur released, potentially exert greater direct and indirect climate forcings.

Acknowledgments: This study was supported by the National Natural Science Foundation of China (21407080), the Foundation Research Project of Jiangsu Province (BK20140987 and BK20150891), the Project Funded by Environmental Science Brand Major of Jiangsu (PPZY2015C222), the Startup Foundation for Introducing Talent (2014r020 and 2015r011), and the open fund by Laboratory/Equipment Management Office of Nanjing University of Information Science and Technology (15KF052 and 15KF053). We also thank the anonymous reviewers for helping to improve the manuscript.

Author Contributions: Zhuang Wang and Se Wang planned and supervised the research, co-wrote the paper; Yiwen Liu performed the theoretical computation, co-wrote the paper; Hao Fang and Degao Wang co-performed the theoretical analysis.

Conflicts of Interest: The authors declare no conflict of interest.

References

1. Zhang, R.; Suh, I.; Zhao, J.; Zhang, D.; Fortner, E.C.; Tie, X.; Molina, L.T.; Molina, M.J. Atmospheric new particle formation enhanced by organic acids. *Science* **2004**, *304*, 1487–1490. [[CrossRef](#)] [[PubMed](#)]
2. Zhang, R.; Khalizov, A.; Wang, L.; Hu, M.; Xu, W. Nucleation and growth of nanoparticles in the atmosphere. *Chem. Rev.* **2012**, *112*, 1957–2011. [[CrossRef](#)] [[PubMed](#)]
3. Zhang, R. Getting to the critical nucleus of aerosol formation. *Science* **2010**, *328*, 1366–1367. [[CrossRef](#)] [[PubMed](#)]
4. Sipilä, M.; Berndt, T.; Petäjä, T.; Brus, D.; Vanhanen, J.; Stratmann, F.; Patokoski, J.; Mauldin, R.L., III; Hyvärinen, A.P.; Lihavainen, H.; *et al.* The role of sulfuric acid in atmospheric nucleation. *Science* **2010**, *327*, 1243–1246. [[CrossRef](#)] [[PubMed](#)]
5. Kulmala, M.; Kerminen, V.M. On the formation and growth of atmospheric nanoparticles. *Atmos. Res.* **2008**, *90*, 132–150. [[CrossRef](#)]
6. Andersen, O. Biodiesel and its blending into fossil diesel. In *Unintended Consequences of Renewable Energy. Problems to be Solved*; Springer: London, UK, 2013; pp. 55–70.
7. Kittelson, D.B.; Watts, W.F.; Johnson, J.P. On-road and laboratory evaluation of combustion aerosols—Part 1: Summary of diesel engine results. *J. Aerosol Sci.* **2006**, *37*, 913–930. [[CrossRef](#)]
8. Kittelson, D.B.; Watts, W.F.; Johnson, J.P.; Schauer, J.J.; Lawson, D.R. On-road and laboratory evaluation of combustion aerosols—Part 2: Summary of spark ignition engine results. *J. Aerosol Sci.* **2006**, *37*, 931–949. [[CrossRef](#)]
9. Kittelson, D.B.; Watts, W.F.; Johnson, J.P.; Remerowski, M.L.; Ische, E.E.; Oberdörster, G.; Gelein, R.M.; Elder, A.; Hopke, P.K.; Kim, E.; *et al.* On-road exposure to highway aerosols. 1. Aerosol and gas measurements. *Inhal. Toxicol.* **2004**, *16*, 31–39. [[CrossRef](#)] [[PubMed](#)]
10. Oberdörster, G. Pulmonary effects of inhaled ultrafine particles. *Int. Arch. Occup. Environ. Health* **2001**, *74*, 1–8. [[CrossRef](#)] [[PubMed](#)]
11. Murr, L.E.; Soto, K.F. A TEM study of soot, carbon nanotubes, and related fullerene nanopolyhedra in common fuel-gas combustion sources. *Mater. Charact.* **2005**, *55*, 50–65. [[CrossRef](#)]
12. Sanchís, J.; Berrojalbiz, N.; Caballero, G.; Dachs, J.; Farré, M.; Barceló, D. Occurrence of aerosol-bound fullerenes in the Mediterranean Sea atmosphere. *Environ. Sci. Technol.* **2012**, *46*, 1335–1343. [[CrossRef](#)] [[PubMed](#)]
13. Wang, Z.; Chen, J.; Sun, Q.; Peijnenburg, W.J.G.M. C₆₀-DOM interactions and effects on C₆₀ apparent solubility: A molecular mechanics and density functional theory study. *Environ. Int.* **2011**, *37*, 1078–1082. [[CrossRef](#)] [[PubMed](#)]
14. Wang, Z.; Tang, L.L.; Peijnenburg, W.J.G.M. Theoretical investigations on C₆₀-ionic liquid interactions and their impacts on C₆₀ dispersion behavior. *Environ. Toxicol. Chem.* **2014**, *33*, 1802–1808. [[CrossRef](#)] [[PubMed](#)]

15. Wang, Z.; Tang, L.L.; Wang, D. Impacts of C₆₀-ionic liquids (ILs) interactions and IL alkyl chain length on C₆₀ dispersion behavior: Insights at the molecular level. *Bull. Korean Chem. Soc.* **2014**, *35*, 2679–2683. [[CrossRef](#)]
16. Wang, Z.; Wang, S.; Chen, M.; Xu, D.; Tang, L.L.; Wang, D. Elucidating adsorption mechanisms of phthalate esters upon carbon nanotubes/graphene and natural organic acid competitive effects in water by DFT and MD calculations. *Bull. Korean Chem. Soc.* **2015**, *36*, 1631–1636. [[CrossRef](#)]
17. Vosko, S.H.; Wilk, L.; Nusair, M. Accurate spin-dependent electron liquid correlation energies for local spin density calculations: A critical analysis. *Can. J. Phys.* **1980**, *58*, 1200–1211. [[CrossRef](#)]
18. Perdew, J.P.; Burke, K.; Ernzerhof, M. Generalized gradient approximation made simple. *Phys. Rev. Lett.* **1996**, *77*. [[CrossRef](#)] [[PubMed](#)]
19. Zhao, J.; Khalizov, A.; Zhang, R.; McGraw, R. Hydrogen-bonding interaction in molecular complexes and clusters of aerosol nucleation precursors. *J. Phys. Chem. A* **2009**, *113*, 680–689. [[CrossRef](#)] [[PubMed](#)]
20. Zhang, R.; Wang, L.; Khalizov, A.F.; Zhao, J.; Zheng, J.; McGraw, R.L.; Molina, L.T. Formation of nanoparticles of blue haze enhanced by anthropogenic pollution. *Proc. Natl. Acad. Sci.* **2009**, *106*, 17650–17654. [[CrossRef](#)] [[PubMed](#)]



© 2016 by the authors; licensee MDPI, Basel, Switzerland. This article is an open access article distributed under the terms and conditions of the Creative Commons by Attribution (CC-BY) license (<http://creativecommons.org/licenses/by/4.0/>).